Alterations in targetable molecular pathways are enriched in *KRAS* wild-type (WT) pancreatic cancer (PC).

Philip Agop Philip[1], Joanne Xiu[2], Michael J. Hall[3], Andrew Eugene Hendifar[4], Emil Lou[5], Jimmy J. Hwang[6], Jun Gong[4], Michelle Ellis[2], Moh'd M. Khushman[7], Davendra Sohal[8], A. Craig Lockhart[9], Benjamin Adam Weinberg[10], John Marshall[10], Axel Grothey[11], Anthony Frank Shields[12], W. Michael Korn[2]

[1]Karmanos Cancer Institute, Detroit, MI; [2]Caris Life Sciences, Phoenix, AZ; [3]Fox Chase Cancer Center, Philadelphia, PA; [4]Samuel Oschin Cancer Center, Cedars-Sinai Medical Center, Los Angeles, CA; [5]University of Minnesota School of Medicine, Minneapolis, MN; [6]Levine Cancer Institute, Charlotte, NC; [7]Medical Oncology, The University of South Alabama, Mitchell Cancer Institute, Mobile, AL; [8]University of Cincinnati, Cincinnati, OH; [9]University of Miami Sylvester Comprehensive Cancer Center, Miami, FL; [10]Georgetown University, Washington, DC; [11]West Cancer Center, Germantown, TN; [12]Karmanos Cancer Institute, Wayne State University, Detroit, MI

CARIS POA™ PRECISION ONCOLOGY ALLIANCE

Abstract #: 4629

Background:

Genomic profiling has identified *KRAS* mutations in 88-90% of PC. *KRAS* WT tumors represent a molecularly heterogeneous group that may harbor targetable alterations. We studied *KRAS* WT PC using NextGen sequencing (NGS) and whole transcriptome sequencing (WTS) in a large cohort of pancreatic tumors to characterize the molecular landscape of this unique group and to assess the prevalence of targetable alterations.

Methods:

- NGS was performed on genomic DNA isolated from FFPE tumor samples using the NextSeq (592-genes) (Illumina, Inc., San Diego, CA).
- All variants were detected with greater than 99% confidence based on allele frequency and amplicon coverage, with an average sequencing depth of coverage of greater than 500 and an analytic sensitivity of 5%.
- A combination of multiple test platforms including NGS, IHC and fragment analysis was used to determine MSI-H/dMMR status.
- Tumor mutational burden (TMB) was estimated from 592 genes (1.4 megabases [MB] sequenced per tumor) by counting all non-synonymous missense mutations found per tumor that had not been previously described as germline alterations.
- IHC was performed on FFPE sections of glass slides. PD-L1 testing was performed using the SP142 (Ventana, Tucson, AZ) anti-PD-L1 clone.
- Gene fusion detection using the Illumina NovaSeq platform (Illumina, Inc., San Diego, CA) and Agilent SureSelect Human All Exon V7 bait panel (Agilent Technologies, Santa Clara, CA).
- Microenvironment Cell Population-counter (MCP-counter) was used for quantification of the abundance of immune and stromal cell population using transcriptomic data. (Becht et al. Genome Biology 2016, 17:218)
- Chi-square and Wilcoxon were used for comparative analyses and Benjamini-Hochberg was used to correct for multiple comparison.

Results:

Table 1: patient characteristics

No significant imbalance in histology, gender or age noted in *KRAS* wild type vs. mutated tumors

	Histology	*KRAS* WT (N)	*KRAS* MT (N)	Total	*KRAS* WT (%)	*KRAS* MT (%)
	All	144	1020	1164		
Histology	**Adenocarcinoma, NOS***	122	943	1065	85%	92%
	Carcinoma, NOS*	14	45	59	10%	4%
	Acinar	3	1	4	2%	0%
	Mucinous	2	12	14	1%	1%
	pseudopapillary	2		2	1%	0%
	spindle	1	2	3	1%	0%
	giant cell		2	2	0%	0%
	Non-small cell		3	3	0%	0%
	PMP		1	1	0%	0%
	Squamous/Adenosquamous		11	11	0%	1%
Gender	**Female**	67	473		47%	46%
	Male	77	547		53%	54%
Age	**Median**	66	67			
	Range	36-92	25-90			

*: NOS, not otherwise specified.

Figure 1: Notable alterations in the 144 *KRAS*-wild type pancreatic tumors

Left: mutations detected; middle: additional alterations detected including Copy number alteration (CNA), MSI/MMR and PD-L1 IHC; right: details of BRAF mutations and categorization based on mechanism of activation

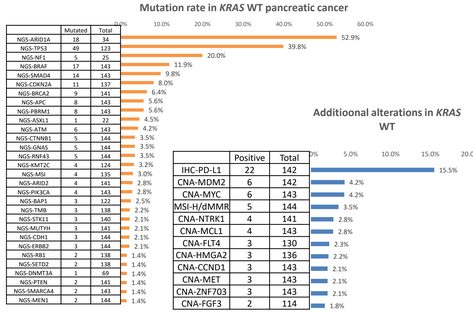

BRAF mutations	Class
V600E	Class 1
V600E	Class 1
V600E	Class 1
V600E	Class 1
V600E	Class 1
V600R	Class 1
G469A	Class 2
K601E	Class 2
L485_A489delinsF	Class 2
N486_P490del	Class 2
N486_P490del	Class 2
N486_P490del	Class 2
T599dup	Class 2
T599dup	Class 2
V600_K601delinsE	Class 2
D594G	Class 3
D594N	Class 3

Figure 2: Oncoprint of the 144 *KRAS*-WT pancreatic tumors.

Colored squares: alteration (mutation, fusion, copy number amplification, IHC overexpression, CISH amplification). Gray squares: no alteration detected. Blank: test not done or indeterminate results.

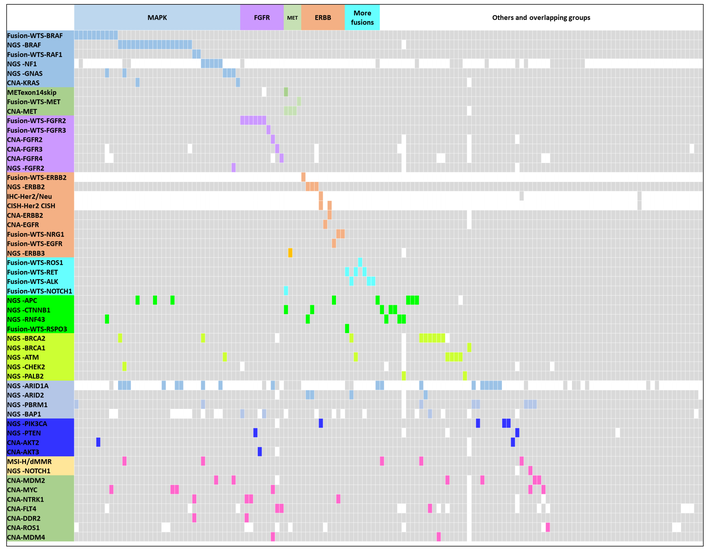

Figure 3: Immune characterization of *KRAS*-WT vs. *KRAS* MT tumors.

Top: PDL1, MSI/MMR and TMB; Middle and Bottom: MCP counter calculated NK and fibroblasts in the tumor microenvironment.

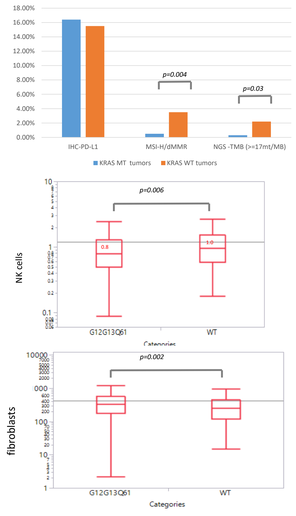

Figure 4:

Volcano plot displaying significance (the higher on the y axis, the smaller the p values) and fold changes (the farther away from 0 on the x axis, the bigger the differences are between *KRAS* vs. WT tumors)

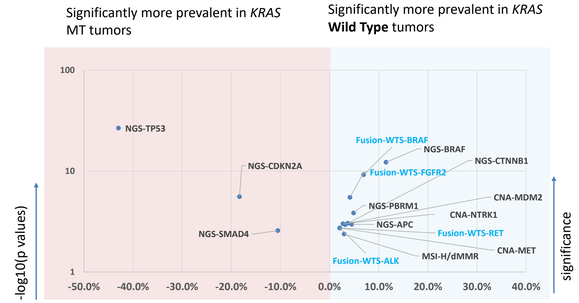

Table 2:

Fusions detected by whole transcriptome sequencing in *KRAS* WT pancreatic cohort

	Fusions	N		Fusions	N
ALK	EML4:ALK	3	MET	MET exon14 skip	1
BRAF	AGAP3:BRAF	2		ST7:MET	1
	BACH1:BRAF	1	NOTCH1	FAM53B:NOTCH1	1
	SND1:BRAF	4	NRG1	ATP1B1:NRG1	2
	TRIM24:BRAF	1	PRKCB	UBFD1:PRKCB	1
	TRIM44:BRAF	1	RAF1	ATG7:RAF1	1
	VPS50:BRAF	1		RRBP1:RAF1	1
EGFR	SEL1L:EGFR	1	RET	EML4:RET	1
FGFR	FGFR2:ALS2CR12	1		ERC1:RET	1
	FGFR2:BICC1	2		NCOA4:RET	1
	FGFR2:SORBS1	1	ROS1	SLC4A4:ROS1	1
	FGFR2:TPM4	1	RSPO3	PTPRK:RSPO3	1
	FGFR2:ZMYM4	1			
	FGFR3:ADD1	1			

Conclusions

- *KRAS* WT PC is significantly more enriched with targetable alterations (e.g., BRAF, ALK, ROS1, NRG1, MSI-H) as compared to *KRAS* MT tumors, suggesting potential benefit of using targeted therapies.
- The use of WTS in combination with NGS identifies activated molecular pathways in the majority of *KRAS* WT tumors.
- Based on our findings, comprehensive profiling of PC at the DNA and RNA level is recommended to provide patients with therapeutic opportunities beyond standard treatments.
- TMB and MSI tend to be higher in *KRAS* WT tumors; microenvironment inferred from WTS using MCP counter suggest more activated innate immunity with a lower fibroblast abundance, suggesting unique immune treatment strategy design.

Reference

- Becht et al. Estimating the Population Abundance of Tissue-Infiltrating Immune and Stromal Cell Populations Using Gene ExpressionGenome Biology (2016) 17:218
- Raphael et al. Integrated Genomic Characterization of Pancreatic Ductal Adenocarcinoma
- 2017, Cancer Cell 32, 185–203